Using Computer Generated Holograms to Test Aspheric Wavefronts

J. C. Wyant and V. P. Bennett

The use of computer generated holograms for the testing of aspheric wavefronts is described. An analysis of the errors produced by emulsion movement, incorrect hologram size and position, and distortion in hologram plotter and photoreduction lens is given, and it is shown that all the errors are proportional to the slope of the aspheric wavefront. Experimental results verifying the error analysis are shown for testing rotationally nonsymmetric wavefronts having slopes as large as 125 waves per radius and departures as large as sixty-five waves.

Introduction

The high performance requirements of modern optical systems have made the inclusion of aspheric surfaces in the design increasingly advantageous. A major obstacle in using aspheric surfaces has been the difficulty involved in accurately testing them.

A common arrangement for testing spherical surfaces is a Twyman-Green interferometer that compares the surface under test with a flat or spherical reference surface. If the surface under test is aspheric, this arrangement is limited in accuracy because the difference between the reference surface and test surface becomes too large. The most common method of solving this problem is to make a second optical system (null lens or null mirror) that converts the wavefront produced by the element under test into either a spherical or a plane wavefront.[1-6] This wavefront can then be interferometrically compared with a spherical or plane reference wavefront. The null optics is often very difficult and expensive to produce. The difficulty and expense become even more severe when nonsymmetric wavefronts are tested.

Clearly, a method of either eliminating or reducing the complexity of null optics is needed. Other papers have indicated that in many cases computer generated holograms (CGH) do provide such a method.[7-10] The purpose of this paper is to give a more detailed analysis of the main sources of error involved in using CGH to test aspheric wavefronts and to support this analysis with experimental results obtained testing nonsymmetric wavefronts.

The CGH this paper is concerned with are basically a binary representation of the actual interferogram that would be obtained if the ideal aspheric wavefront being tested were interfered with a tilted plane wavefront. This can be understood more clearly if the procedure for making and using a hologram is looked at.

The experimental setup that would be used to test an aspheric wavefront using a CGH is essentially the same setup that would be used to perform the test without the CGH. For example, Fig. 1 shows what is essentially a Twyman-Green interferometer used to test an aspheric mirror. The hologram is placed in the image plane of the mirror under test, i.e., in the same position film would be placed if a recording were to be made of the interference of the aspheric wavefront produced by the mirror under test with the reference wavefront. The procedure for making the CGH would be to first raytrace the interferometer to determine the position of the fringes in the theoretical interferogram that would be obtained if the mirror under test were perfect. A plotter is then used to draw lines along the calculated fringe positions. This plot is photoreduced to the same size as the theoretical interferogram.

When the CGH is placed in the interferometer as shown in Fig. 1, the CGH and the interference fringes produced by the interference of the reference wavefront and the wavefront produced by the mirror under test produce a moire pattern that gives the difference between the CGH and the interference fringes. Spatial filtering can be used to improve the contrast of the moire pattern. Spatial filtering is accomplished by reimaging the hologram with an appropriately placed small aperture in the focal plane of the reimaging lens. This aperture is placed such that it passes only the wavefront from the mirror under test and the corresponding wavefront produced by illuminating the hologram with a plane wavefront. The requirement for being able to accomplish this spatial filtering is that in the making of the CGH, the slope (tilt) of the plane reference wavefront is at least as large as the maximum slope of the aspheric wavefront along the intersection

Both authors were at Itek Corporation, Optical Systems Division, Lexington, Massachusetts 02173, when this work was done; V. P. Bennett is now at the Institute of Optics of the University of Rochester.

Received 28 June 1972.

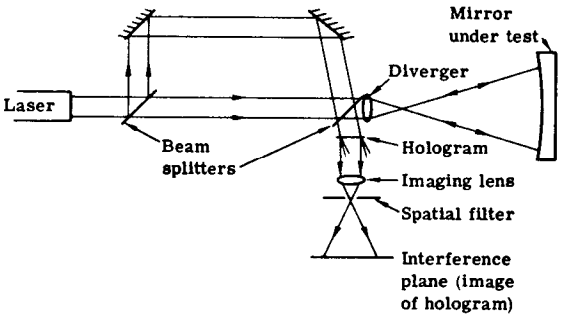

Fig. 1. Modified Twyman-Green interferometer.

Table I. Main Source of Error in CGH to Test Aspheric Wavefronts

.Emulsion movement
.Plotter distortion
. Photoreduction lens distortion
. Incorrect hologram size
. Misalignment of hologram in interferometer

of the plane of incidence of the plane wave and the aspheric wavefront. Thus, in the interference plane shown, an interferogram is produced that gives the difference between the wavefront produced by the mirror under test and the corresponding wavefront produced by the hologram.

There are obviously many places in the interferometer where a CGH could be placed. The major reason it is placed as shown is that thickness variations in the hologram plate have no effect on the results, and thus what could be a very serious source of error is eliminated.

It should be stressed that the above raytracing procedure used to make the holograms can be used for any general optical system. The only requirement is that all the optics in the interferometer be known so the system can be raytraced. An important consequence of raytracing the entire interferometer is that even though the diverger may be corrected only for spherical wavefronts and may introduce additional aberrations in the aspheric wavefront being passed through it, the hologram automatically corrects for these aberrations when a null test (or for all practical purposes, a near null test) is performed.

Error Analysis

Table I shows the main sources of error involved in using a CGH to test an aspheric wavefront.

To determine the error produced by emulsion movement, 25-mm diam holograms of two collimated wavefronts were made on Kodak 649-F plates. The holograms were developed in Kodak HRP for 5 min, after which they were put in an acetic stop bath for 15 sec and Kodak fixer for 3 min. They were washed in running water for 5 min and rinsed for 30 sec in Yankee instant film dryer and conditioner and air dried.

After processing, the hologram was replaced back into the original setup, and one of the original collimated wavefronts was interfered with the corresponding wavefront reconstructed by the hologram. Interferograms were recorded, and the average rms and peak wavefront errors measured for the three spatial frequencies investigated are shown in Table II. Three holograms were made at each of the three spatial (carrier) frequencies.

It is not believed that the wavefront errors shown in Table II were predominately a result of emulsion movement since the magnitude of the error does not appear to be largely dependent upon the spatial frequency of the hologram fringes.. Emulsion movement is probably partly dependent upon spatial frequency of the recorded fringe pattern, but it is unlikely that this dependence would be large enough to nearly cancel out the result that the peak error produced by a given emulsion movement should increase at the same rate as the spatial frequency of the recorded fringes. Other possible sources of error are noise produced by dust in the collimated wavefronts, small error in repositioning of the hologram, turbulence, and what is believed to be the largest source of error, noise in data reduction process. The important conclusion is that the rms error produced by emulsion movement is certainly less than $\lambda/40$.

The next source of error to be investigated is distortion in the-hologram plotter. To show how the CGH wavefront accuracy depends upon the number of distortion free plotter resolution points and the maximum slope of the aspheric wavefront being tested, let us suppose the plotter has P X P resolution points. Thus, there are $P/2$ resolution points across the radius of the hologram. Since by definition the maximum error in plotting any point is one-half of a resolution unit, any portion of each line making up the hologram could be displaced from where it should be a distance equal to l/P the radius of the hologram. Let the maximum difference between the slope of the aspheric wavefront and the tilted plane wave be S waves per hologram radius. Thus, the phase of the plane wave at the hologram lines. can differ from that of the required wavefront at the same lines by as much as

$$2\pi \text{ (S/P) rad or S/P waves.} \qquad (1)$$

Therefore, in the hologram plane the error in the reconstructed wavefront-can be as large as S/P waves. Since the final interferogram is recorded in the image plane of the hologram, the quantization due to the finite number of resolution points causes a peak error-in the final interferogram of S/P waves. Figure 2 is a

Table II. Average rms and Peak Error in Wavefront Produced by Hologram

Spatial freq. of hologram fringes	Average rms error	Average peak error
40 l/mm	0.025X	0.073x
330 l/mm	0.021x	0.061X
1000 l/mm	0.023X	0.065X

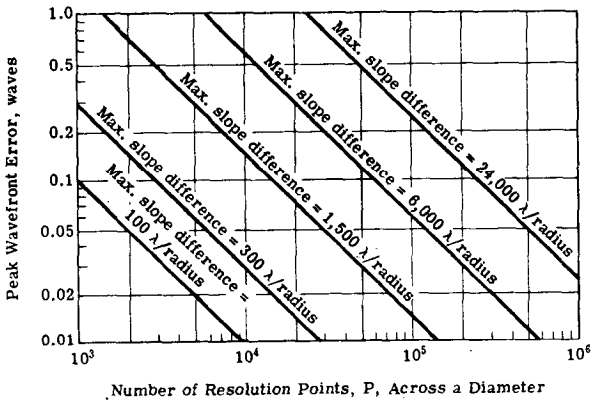

Fig. 2. Peak wavefront error vs. number of plotter resolution points.

log-log graph of peak wavefront error vs number of plotter resolution points for various amounts of maximum difference between the slope of the aspheric wavefront and the slope of the tilted plane wave.

As mentioned above, to maximize the contrast of the final interferogram, the hologram should be made such that it is possible to spatially filter the hologram to select out the first order reconstruction. This requires that the slope (tilt) of the plane reference wavefront is at least as large as the maximum slope of the aspheric wavefront along the intersection of the plane of incidence of the plane wave and the aspheric wavefront. The larger the slope of the plane reference wavefront, the easier it is to select out the first order reconstruction. However, increasing the slope of the plane reference wavefront decreases the accuracy of the aspheric wavefront produced. In the testing of nonsymmetric wavefronts, advantage should be taken of the fact that a smaller reference wavefront tilt can be used if the plane of incidence of the reference wavefront is along the direction of minimum slope of the aspheric wavefront.

In an effort to verify results shown in Fig. 2, three different CGH were made to produce spherical wavefronts having maximum slopes of 50, 100, and 200 waves/radius, Spherical wavefronts were selected because they are easy to test accurately. The slope of the reference plane wavefront was selected such that maximum difference between the slope of the spherical wavefronts and the slope of the plane wave was 150, 300, and 600 waves/radius. The spherical wavefronts produced by the holograms were interfered with spherical wavefronts produced by high quality (peak wavefront error less than 0.05 wave) wavefronts. The experimental setup was shown in Fig. 1, except that both the diverger and spherical mirror were of known high quality, and the spacing between the diverger lens and mirror was adjusted to obtain the desired sphericity to match the wavefront produced by the hologram. Table III shows the peak wavefront errors obtained testing the three holograms.

If the Calcomp model 736 plotter used to make the holograms had a known number of resolution points, a comparison could be made between the measured peak wavefront errors and the values calculated using Eq. (1). Unfortunately, the Calcomp plotter does not have a known number of distortion free resolution points. It has 6000 X 6000 resolution points, but they are not distortion free. What can be done is to use Eq. (1) and the measured values of peak wavefront error to calculate a value of distortion free resolution points, *P*, for each value of the slope, S, investigated. The results are shown in Table III.

Table III shows that approximately the same number of distortion free resolution points is calculated for the three values of S investigated. Thus, the experimental results indicate that over the limited range of S investigated the peak wavefront error is approximately proportional to the maximum difference between the slope of the wavefront produced and the tilted plane wavefront. Although it is not strictly proven, it appears as though the Calcomp plotter has in the neighborhood of 1500 distortion free resolution points across a diameter.

The above results indicate, but do not definitely prove, that Fig. 2 is correct. To really verify Fig. 2, a larger range of S must be investigated and *P* must be determined by some independent manner. In order to extend the range of S, a plotter having many more resolution points than the Calcomp plotter must be used.

The next source of error to be investigated is the error due to incorrect hologram size. Let Ø(r, θ) be the aberrated wavefront being tested in the plane of the hologram. If the hologram is the correct, size, this is the wavefront the hologram produces. If the hologram has the incorrect size by magnification factor, M, the test gives the difference Ø(r/M, θ) - Ø(r, θ). Now by a Taylor's expansion,

$$\vartheta\left(\frac{r}{M},\theta\right)=\vartheta\left[r+\left(\frac{1}{M}-1\right)r,\theta\right]=\vartheta(r,\sigma)+\frac{\partial\vartheta(r.\theta)}{\partial r}\left(\frac{1}{M}-1\right)r+\cdots \quad (2)$$

Terms higher than first order in the expansion can be neglected if M is sufficiently close to 1 and a small region is looked at.

Thus, the error in the test results caused by the hologram having the incorrect size is given by

$$\vartheta\left(\frac{r}{M},\theta\right)-\vartheta(r,\theta)=\frac{\partial\vartheta(r,\theta)}{\partial r}\left(\frac{1}{M}-1\right)r+\cdots \quad (3)$$

Table III. Results of Testing Spherical Wavefronts Produced by CGH

Max. slope difference, S (waves/radius)	Avg. peak wavefront error	Calculated number of distortion free resolution points, *P*
600	0.40λ	1500
300	0.24λ	1250
150	0.10λ	1500

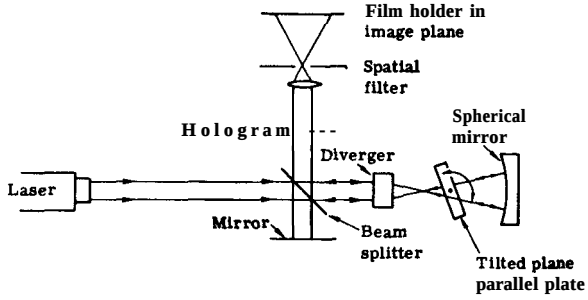

Fig. 3. Experimental setup to obtain nonsymmetric aspheric wavefront.

If $\partial \Phi / \partial r$, the radial slope, has units of waves per radius, r becomes the normalized radius.

A distortion error is analyzed the same as a magnification error except that the magnification, M, is a function of position r. Let $\alpha(r)$ be the distortion as a function of radius ***r.*** That is, a point that is supposed to be at a radius ***r*** is at a radius $r[1 + \alpha(r)]$. Since often in a test both the distortion and wavefront slope are maximums at the maximum value of ***r,*** the error due to distortion can be reduced by adjusting the magnification to balance out the distortion error at the edge of the plot. That is, the photoreduction should be demagnified by a factor $1 + \alpha(r_{max})$ from what it would be if no distortion were present. Thus, the magnification error due to distortion at any radius r is

$$M(\alpha) = [1 + \alpha(r)]/[1 + \alpha(r_{max})]. \quad (4)$$

Error due to misalignment of hologram in interferometer could be due to either an off-center error or, in the case of testing nonsymmetric wavefronts, a rotation error. The off-center error will be looked at first.

Let $\Phi(x,y)$ be the wavefront being tested. Let the center of the aberrated wavefront and the center of the hologram be displaced a distance Δ_x in the x direction. Then the result of the interference test gives $\Phi(x + \Delta x, y) - \Phi(x,y)$. Just as before, a Taylor series expansion leads to

$$\vartheta(x + \Delta x, y) - \vartheta(x,y) \approx [\partial \vartheta(x,y)/\partial x]\Delta x. \quad (5)$$

Equation (5) gives the error resulting from off centering the hologram a distance Δx; $\partial\phi/\partial x$ is just the slope in the x direction. If the units are picked as waves per radius, Ax is the fractional part of the total radius that the hologram is displaced.

When nonrotationally symmetric wavefronts are being tested, an error will result when the hologram has an incorrect rotational position. Again writing Φ in polar coordinates, i.e., $\Phi(r, \theta)$, the test gives the difference $\Phi(r, \theta + \Delta\theta) - \Phi(r, \theta)$, where $\Delta\theta$ is the angular error. The Taylor series expansion gives

$$\vartheta(r,\theta + \Delta\theta) - \vartheta(r,\theta) \approx [\partial \vartheta(r,\theta)/\partial\theta]\Delta\theta. \quad (6)$$

Thus, Eq. (6) is the error that results from an angular error; $\partial \Phi(r, \theta) / \partial \theta$ is the angular slope. If it is measured in waves per radians, $\Delta\theta$ must of course be measured in radians.

Test of Aspheric Nonsymmetric Wavefronts

Figure 3 shows the experimental setup used to obtain a known aspheric nonsymmetric wavefront. The amount of aberration in the wavefront being tested was selected by tilting the plane parallel plate placed between the diverger and spherical mirror. All the optical components in the setup were tested and found to have a peak error less than 1/20th wave except for the diverger. In double pass, the diverger has a 1/8th wave peak error.

To make the desired hologram to test the optical system shown in Fig. 3, the system must first be ray traced. A computer program was written to obtain the position of the fringes in the hologram plane that result from the interference of the tilted plane wave and the aspheric wavefront. The program locates the fringe position by iteration to any desired accuracy and outputs the sequential positions along a fringe onto a tape. Another computer program uses the data written on the tape to generate a 71-cm diam hologram on the Calcomp model 736 plotter. The hologram is plotted one fringe at a time, and parabolic interpolation is used to produce smooth fringes. To achieve wide fringes, each one is traced a number of times, usually five, with a small lateral shift introduced. The resultant plot consists of wide dark fringes against a white background. A typical computer plot is shown in Fig. 4. The total computer time on a CDC 3300 used to produce one hologram is approximately 20 min, and plotter time is about 10 h.

The 71-cm diam computer plot was photoreduced to the correct size of approximately 1.2 cm in diameter with a f/3, 39-mm focal length, Nikon lens. The photographic process described earlier was used.

For all our tests, the spatial filter shown in Fig. 3 was positioned such that the final interferogram showed the interference between the aberrated wavefront pro-

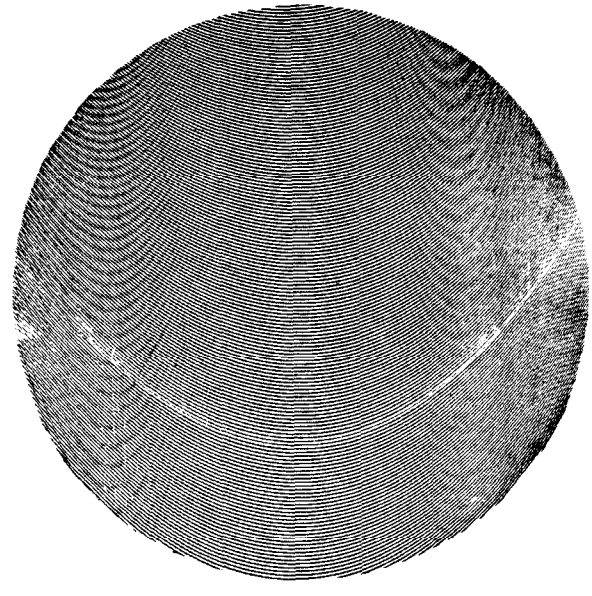

Fig. 4. Typical computer plot.

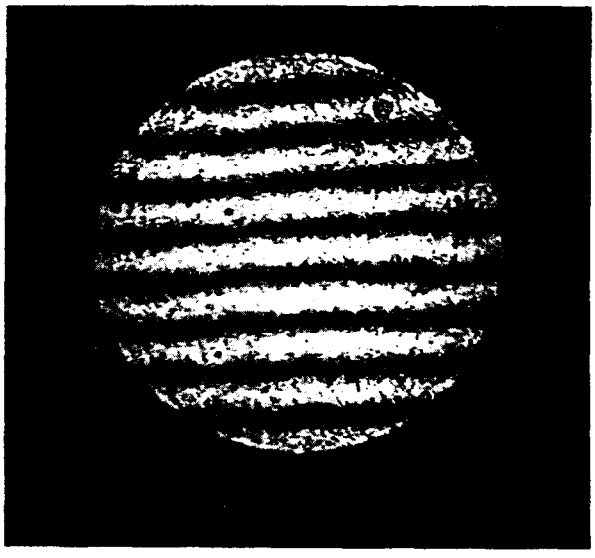

(a)

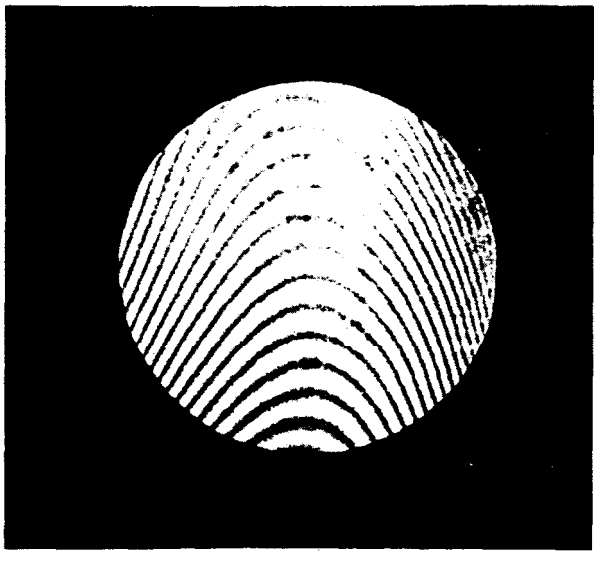

(b)

Fig. 5. CGH test of aspheric wavefront having a maximum slope of thirty-five waves per radius and nineteen waves departure. (a) Results of CGH test. (b) Interference of aberrated wavefront and plane wave.

duced by the optical system and the aberrated wavefront produced by the hologram. The same results would have been obtained if the spatial filter were positioned so as to pass the plane reference wave and the plane wavefront produced by the hologram when the aberrated wavefront is used as the reconstructing beam.

Figures 5 and 6 show typical interferograms resulting from the CGH testing of the nonsymmetric aspheric wavefronts obtained using the setup shown in Fig. 3. The ideal result would of course be equispaced straight fringes. Also shown in the figures are the interferograms obtained by interfering the aspheric wavefronts with a tilted plane wave. Table IV summarizes the experimental results.

The most difficult part of the experiment was the alignment, of the hologram with the aberrated wavefront. To aid in the centering of the hologram, the plotter drew a circle around the circumference of the plot. The circle was a little hard to see in the photoreduction, so black tape was also placed on the circumference of the plot. In the photoreduction the black tape shows up as a low density region around the higher density hologram. The aberrated wave in the image plane was 12.6 mm in diameter, and the hologram was 12.2 mm in diameter so it was easy to see the overlap in the low density black tape region. Experimental results gave a standard deviation of 0.01 mm in centering the hologram. Thus Eq. (5) can be used to calculate an approximate error due to the hologram being off centered. As an example, consider the 20° hologram.

(a)

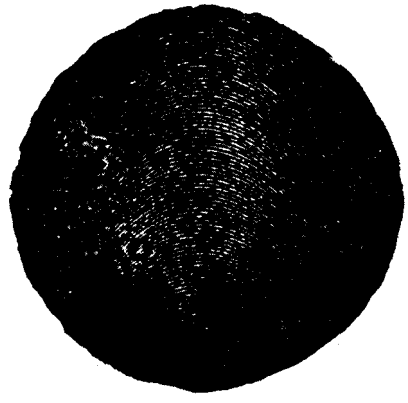

(b)

Fig. 6. CGH test of aspheric wavefront having a maximum slope of 126 waves per radius and sixty-four waves departure. (a) Results of CGH test. (b) Interference of aberrated wavefront and plane wave.

Table IV. Summary of Experimental Results

Tilted plate angle	Maximum slope of aspheric wavefront in units of λ/radius	Maximum departure of aspheric wavefront from a spherical wavefront	rms error of CGH test	Peak error of CGH test
20°	24 λ/R	12.54 λ	0.04 λ	0.13 λ
25°	35 λ/R	19.16 λ	0.05 λ	0.15 λ
30°	56 λ/R	30 λ	0.05 λ	0.15 λ
35°	77 λ/R	40 λ	0.07 λ	0.20 λ
40°	100 λ/R	51.6 λ	0.06 λ	0.17 λ
45°	126 λ/R	64 λ	0.07 λ	0.22 λ

As Table IV shows, the maximum slope of the aberrated wavefront is twenty-four waves per radius. Since the radius of the hologram is 6.10 mm, and the standard deviation of the error in centering the hologram is 0.01 mm, the fractional part of the total radius the hologram is displaced is 0.01/6.1 = 0.00164. Thus Eq. (5) gives the error as (0.00164) (twenty-four waves) = 0.038 waves. The errors for the other holograms are shown in Table V.

To obtain proper angular orientation of the hologram a line is drawn along the vertical edge of the computer plot. If the hologram is correctly placed in the interferometer, the image of the line is parallel to the rotation axis of the tilted plate. The rotation axis of the plate and the image of the line were both made vertical to within an error of approximately 0.004 rad. Thus, Eq. (6) can be used to calculate the error in the test that results from the angular error. As an example, the 20° hologram case will be looked at.

For this case, the maximum angular slope, $\partial\phi/(\partial\theta)$ was found to be approximately 11.8 waves/rad. Thus, the maximum error due to incorrect angular orientation of the hologram is approximately (11.8 waves/rad) (0.004 rad) = 0.047 λ. The errors for the other holograms are also shown in Table V.

A third error results from the hologram having an incorrect size. The diameter of the photoreduced hologram was measured on an electronic comparator. Experimental measurements gave a standard deviation in the measurements of 0.025 mm. For a 12.225 mm diam hologram this gives a magnification error, M, of 12.25/12.225 = 1.0002 or 12.20/12.225 = 0.9998. Thus, [(l/M) - l] = ±0.0002.

Table IV gives the maximum radial slope of the wavefront being tested for the 20° hologram case of twenty-four waves/radius. Using Eq. (3), the peak error resulting from incorrect hologram size for the 20° hologram case is equal to (twenty-four waves) (0.0002) = 0.0048 λ. Results for the other holograms are shown in Table V.

To calculate the error due to distortion in the photoreduction lens, the distortion as a function of radius, *r*, must be known. The data supplied with the photoreduction lens used in the experiment show that at the approximate conjugates and for the maximum field angle used, the maximum distortion is approximately 0.05%. Unfortunately, only the maximum distortion was given, and no information was supplied on how the distortion varied with field angle. Thus, Eqs. (3) and (4) cannot be used to calculate the error due to distortion. To set an upper limit on the distortion error, a calculation of the error was made assuming that maximum distortion occurs at the position of maximum radial slope of the wavefront being tested. That is, M = (1 + 0.0005) and the maximum values of $\partial\theta/\partial$ r given in Table IV were substituted in Eq. (3) to calculate the distortion errors given in Table V. These errors are probably a half-order of magnitude larger than what actually existed.

The last error to be calculated is the error resulting from inaccuracies in the hologram plotter. Equation (1) could be used to calculate the peak error if the number of plotter resolution points were known. This number is not known for sure, but the results shown above indicate that the number is in the neighborhood of 1500 points. Thus, this number will be used in the calculations.

Table IV gives the maximum slope of the six wavefronts tested. S in Eq. (1) is the maximum difference between the slope of the aspheric wavefront and the slope of the reference plane wavefront. To minimize the difference between the slope of the aspheric wavefront and reference plane wavefront, the orientation of the plane incidence of the reference plane wave was selected such that the axis of minimum radial slope was in the plane of incidence.

For all holograms the slope of the plane reference wavefront was eighty waves/radius. Thus, S, the maximum difference between slope of the aspheric wavefront and slope of the reference plane wavefront was either approximately eighty waves/radius or the maximum slope of the aspheric wavefront, whichever was the larger. Table IV shows that S was eighty waves/radius for the 20°, 25°, 30°, and 35° holograms and 100 or 126 waves/radius for the 40° and 45° holograms, respectively. Using these values of S and a value for P of 1500 resolution points, Eq. (1) was used to calculate the peak error to plotter inaccuracy shown in Table V.

All the measured errors shown in Table IV are within the estimated errors in the experiment. At first, it might appear as though the measured errors in the smaller aberration wavefront tests are a little too large,

Table V. Estimate of Peak Errors

Tilted plate angle	Magnification error	Off-center error	Rotation error	Distortion error	Plotter error
20°	0.0048 λ	0.038 λ	0.047 λ	0.012 λ	0.053 λ
25°	0.0070 λ	0.056 λ	0.064 λ	0.017 λ	0.053 λ
30°	0.0112 λ	0.091 λ	0.107 λ	0.028 λ	0.053 λ
35°	0.0154 λ	0.124 λ	0.161 λ	0.038 λ	0.053 λ
40°	0.0198 λ	0.159 λ	0.196 λ	0.050 λ	0.066 λ
45°	0.0252 λ	0.0207 λ	0.257 λ	0.063 λ	0.084 λ

but it must be remembered that the diverger had better than 0.1 wave peak error when used in double pass. This aberration was evident in all the CGH interferograms and is responsible for a large part of the errors in the smaller aberration wavefront tests. It is very satisfying that the larger aberration wavefront test errors are as small as they are and that they are within the estimated errors given in Table V.

All the estimated errors shown in Table V are proportional to the maximum aspheric wavefront slope in either the radial or angular direction. The error due to plotter inaccuracy can only be reduced by using a plotter having more resolution points. The error due to distortion in the photoreduction lens could of course be reduced by using a lens with a maximum distortion of less than 0.05%. However, it should be remembered that the errors due to distortion given in Table V are most likely at least a factor of 5 larger than the actual values. The errors due to incorrect hologram size and incorrect positioning of the hologram were determined by the smallest distance that could be measured in the hologram plane. If the hologram size were increased, the smallest distance that. could be measured in the hologram plane would remain essentially constant. Thus, the errors due to incorrect hologram size and incorrect hologram position would decrease as the size of the hologram increased. If the hologram diameter were increased from 12.7 mm to 50.8 mm these errors would decrease by about a factor of 4. Thus, in the future a CGH test setup should be designed such that the hologram can be as large as possible.

It should also be mentioned that the errors due to incorrect hologram size and position are random errors and could be reduced by repeating the experiment many times and averaging.

Conclusions and Summary

The results given in this paper indicate that CGH can in many instances be used to either eliminate or reduce the complexity of null optics for the testing of both symmetric and nonsymmetric aspheric wavefronts. Probably their greatest use will come in replacing complicated null optics with simple null optics and a CGH. The error analysis given above can be used to calculate before the test the approximate errors in the experiment to determine if adequate accuracy will be obtained. The error due to distortion in the photographic lens is not felt to be a limiting factor at the present time. Errors due to incorrect hologram size or position can be reduced by making the hologram larger or by repeating the test several times. However, error due to plotter inaccuracies can be reduced only by using a more accurate plotter. We are presently investigating the use of a laser beam recorder, which has only approximately the same number of distortion free resolution points as the presently used plotter. Most of the distortion is repeatable so it can be removed in the software, and it is hoped that almost an order of magnitude more resolution points will be obtained.

The authors thank P. K. O'Neill for his many helpful contributions and C. King, S. Lerman, and M. Hurwitz for the development of the computer programs.

References

1. A. Offner, Appl. Opt. 2, 153 (1963).
2. A. B. Meinel, ***Technical Report I, Introduction to Design of Astronomical Telescope*** (University of Arizona Press, Tucson 1965), p. 66.
3. R. Hilbert and M. Rimmer, J. Opt. Soc. Am. 59 ,485 (1969).
4. R. E. Fischer, J. Opt. Soc. Am. 61, 655 (1971).
5. W. J. Smith, Appl. Opt. l0, 2389 (1971).
6. R. E. Parks, J. Opt. Soc. Am. 62, 726 (1972).
7. J. Pastor, Appl. Opt. 8, 525 (1969).
8. J. Pastor, J. S. Harris, and G. E. Evans, J. Opt. Soc. Am. 58, 1556A (1968).
9. A. J. MacGovern and J. C. Wyant, Appl. Opt. 10, 619 (1971).
10. J. C. Wyant and A. J. MacGovern, International Symposium Application de I'Holographie, Besancon, France, July 1970.